Global Change Biology (2000) **6,** 709–725

A global prognostic scheme of leaf onset using satellite data

A. BOTTA,* N. VIOVY,† P. CIAIS,† P. FRIEDLINGSTEIN† and P. MONFRAY†
Centre for Sustainability and the Global Environment (SAGE), Institute for Environmental Studies, University of Wisconsin, 1225 W Dayton street, Madison, WI 53706, USA, †Laboratoire des Sciences du Climat et de l'Environnement (LSCE), CE l'orme des merisiers, 91191 Gif-sur-Yvette, France

Abstract

Leaf phenology describes the seasonal cycle of leaf functioning. Although it is essential for understanding the interactions between the biosphere, the climate, and biogeochemical cycles, it has received little attention in the modelling community at global scale. This article focuses on the prediction of spatial patterns of the climatological onset date of leaf growth for the decade 1983–93. It examines the possibility of extrapolating existing local models of leaf onset date to the global scale. Climate is the main variable that controls leaf phenology for a given biome at this scale, and satellite observations provide a unique means to study the seasonal cycle of canopies. We combine leaf onset dates retrieved from NOAA/AVHRR satellite NDVI with climate data and the DISCover land-cover map to identify appropriate models, and determine their new parameters at a 0.5° spatial resolution. We define two main regions: at temperate and high latitudes leaf onset models are mainly dependent on temperature; at low latitudes they are controlled by water availability. Some local leaf onset models are no longer relevant at the global scale making their calibration impossible. Nevertheless, we define our unified model by retaining the model that best reproduced the spatial distribution of leaf onset dates for each biome. The main spatial patterns of leaf onset date are well simulated, such as the Sahelian gradient due to aridity and the high latitude gradient due to frost. At temperate and high latitudes, simulated onset dates are in good agreement with climatological observations; 62% of treated grid-cells have a simulated leaf onset date within 10 days of the satellite observed onset date (which is also the temporal resolution of the NDVI data). In tropical areas, the subgrid heterogeneity of the phenology is larger and our model's predictive power is diminished. The difficulties encountered in the tropics are due to the ambiguity of the satellite signal interpretation and the low reliability of rainfall and soil moisture fields.

Keywords: global modelling, leaf phenology, onset date, satellite NDVI

Received 21 May 1999; resubmitted and accepted 15 December 1999

Introduction

Phenology is the study of the timing of recurrent biological events and the causes of timing with regard to biotic and abiotic forces (Lieth 1975). This article focuses on leaf phenology in general, and on the climatological onset of leaf growth, in particular. Usually defined as the time evolution of the leaf-area index (LAI), leaf phenology depends primarily on the climatic conditions for a given biome. It strongly affects land-surface boundary conditions and the exchange of matter and energy with the atmosphere, influencing the surface albedo, roughness, and dynamics of the terrestrial water cycle. Changes in the phase of LAI evolution may therefore have impacts on climate (Chase *et al.* 1996; Betts *et al.* 1997; Botta 1999). Leaf phenology also affects the terrestrial carbon cycle. Myneni *et al.* (1997) and Menzel & Fabian (1999) have recently highlighted the importance of ongoing large-scale changes of phenology. Besides, Goulden *et al.* (1996) have correlated changes in

Correspondence: Aurélie Botta, tel +1/608 2624775, fax +1/608 2634190, e-mail adbotta@facstaff.wisc.edu

phenology with variations in carbon uptake at the stand level

Therefore, it is crucial to account for changes in phenology to accurately simulate seasonal cycles in coupled biosphere/atmosphere climate models, in terrestrial biogeochemical cycle models, and in vegetation dynamics models. To date, the leaf onset date of such models has been either prescribed (Ruimy *et al.* 1996; Sellers *et al.* 1996) or parameterized using very simple methods (Haxeltine & Prentice 1996). In some cases, these parameterizations have been tested against phenological observations, but generally only for mid and high latitudes (Kaduk & Heimann 1996; Friend *et al.* 1997). More realistic leaf onset models based on plant physiological principles developed at the stand level have recently been extrapolated for the United States by White *et al.* (1997). However, very little work has been carried out so far on leaf onset in arid and semiarid regions, where phenology is controlled predominantly by water availability. The aim of the present study is to use satellite observations to extrapolate different process-based phenological models established at the stand level, and reproduce the global-scale spatial distribution of the climatological leaf onset date for 1983–93.

In the following section, we describe the input datasets, the land-cover map, the leaf onset date retrieved from the temporal evolution of the NDVI index, and the gridded climate and soil moisture fields. In the second section, we review the leaf onset models applied previously at the stand level for different vegetation types or biomes. We then construct one or several models for each biome and calibrate them using climate data and satellite onset dates averaged for 1983–93 at a 0.5° spatial resolution. In the final section, we define our global unified model by incorporating the stand-level models that best reproduce the spatial variability of leaf onset date for each biome.

Input datasets

Both the land-cover map and the global leaf onset dates are retrieved from satellite observations, using primary NOAA/AVHRR measurements.

The land-cover map

In order to establish a land-cover map consistent with the satellite dataset used to infer the observed leaf onset dates, we chose the DISCover global land-cover dataset (Loveland & Belward 1997). This dataset was derived using monthly NDVI from 1992 to 1993 1-km AVHRR. It distinguishes 14 vegetation types and 2 types of bare soil. We determine the dominant vegetation type first at 8-km resolution and then at 0.5° resolution, the working resolution of our unified onset date model. Because a single vegetation type covers more than 50% of the surface in 86% of the 0.5° pixels, we expect spatial aggregation to retain most of the original information. Figure 1(a) shows the DISCover map aggregated at 0.5° resolution.

We excluded the evergreen broadleaf forest biome from our analysis as it has little or no leaf seasonal cycle. We also excluded croplands, whose phenology depends largely on management practices (e.g. irrigation, fertilization) and crop types. However, we included the mixed biome crop/natural vegetation mosaic, assuming that natural vegetation dominates the satellite-derived phenological signal. We focused our attention on deciduous biomes; however, the DISCover classification of deciduous contains areas where no seasonal cycle is detected by satellite imagery. For example, the open shrubland biome constituted by scrubs and grasses mixed with bare soil is deciduous, but the seasonality of its NDVI cycle is too low to detect an onset date over 62% of its surface at a 0.5° resolution. Such pixels are therefore excluded from the study. Conversely, the evergreen needleleaf forest biome exhibits a pronounced NDVI seasonal cycle. This cycle is due predominantly to changes in snow cover, but it is also linked to the leaf onset of the deciduous understorey and to an increase in the photosynthetic activity of conifer needles. A comparison with dates of snow melt sensed remotely from the SSM/I instrument demonstrated that the snow cover always disappears several days before the leaf onset date retrieved from NDVI evolution (Botta 1999). Thus, we assume that the onset date detected in the NDVI is due to leaf phenology, and we included this biome in our analysis.

In the DISCover classification a single biome may exist both in tropical and boreal regions (e.g. woody savannah in Fig. 1a). To study phenology, we need to subdivide biomes according to their climate regime in order to define and apply the suitable model. To do so, we first separate biomes where temperature controls the onset date from biomes where other factors, predominantly water availability, also intervene. In the following, we use the terms 'temperature controlled' and 'water controlled' to refer to this distinction. We base the subdivision on three climate criteria: the annual mean of the daily mean temperature (T_{mean}), the coldest daily mean temperature of the year (T_c), and the annual range in daily temperature ($\Delta_T = T_w - T_c$, where T_w is the warmest daily mean temperature of the year). According to the region, the prefix 'cool' or 'warm' is added to the biome name (Table 1). Some partitions are obvious, such as for woody savannahs or closed shrublands. Others as for grasslands or mixed forests are more arbitrary.

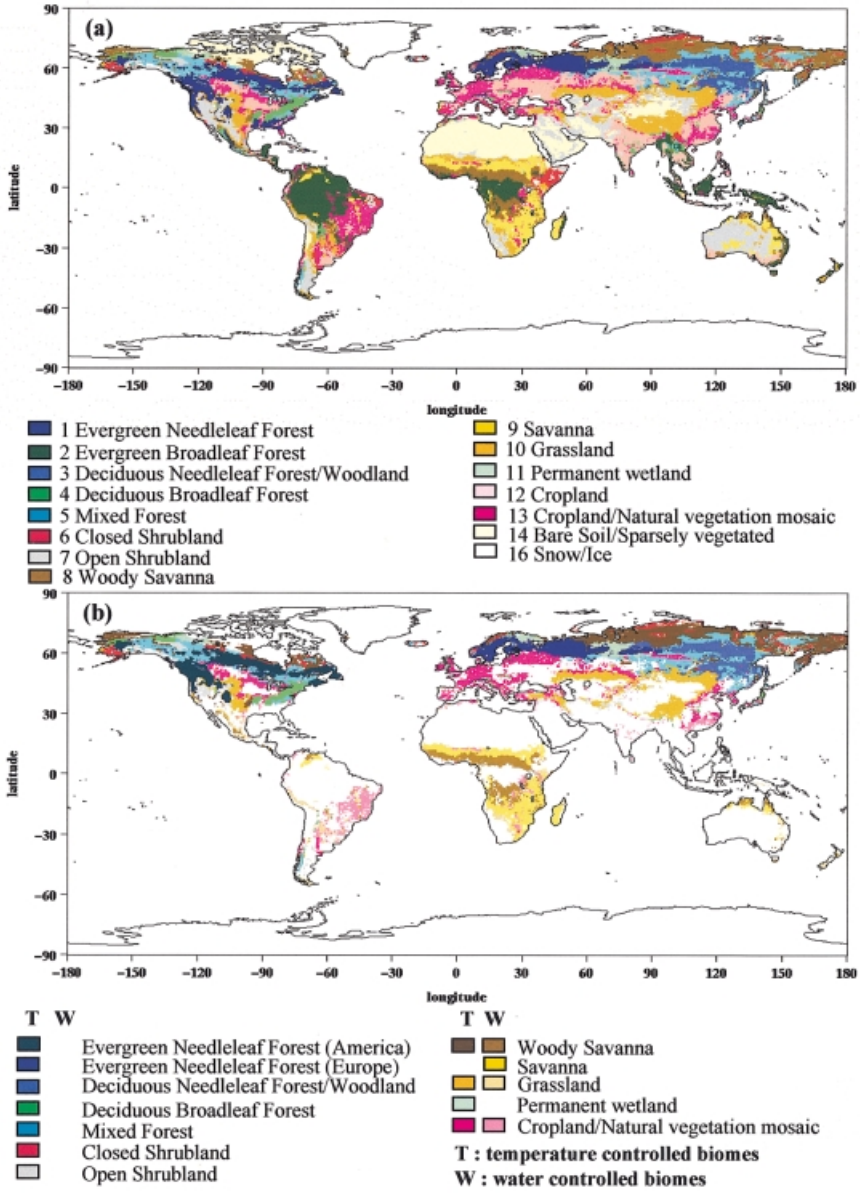

Fig. 1 DISCover global land-cover map retrieved from satellite observations and ground measurements (Loveland & Belward 1997). Initially at 1-km resolution, this classification is aggregated at a 0.5° resolution by retaining the major land-cover for: (a) all biomes; (b) redefined biomes (white areas are either excluded biomes like croplands, or areas with no seasonal cycle detectable by satellite).

The leaf onset inferred from satellite measurements

The NDVI is the difference between near-infrared and visible reflectance of land-surface normalized by their sum. The differential response of vegetation and bare soil characterizes the phenological state of vegetation (Rouse *et al.* 1974; Justice *et al.* 1985). We used the NOAA-AVHRR Pathfinder dataset with a 10-day time-step and an 8-km spatial resolution (Townshend 1994). The data were corrected using the Best Index Slope Extraction (BISE) algorithm, in order to reduce the effect of cloud contamination, atmospheric interference, and bidirectional reflectance (Viovy *et al.* 1992).

The method for determining the leaf onset date from the NDVI time-series is described in Moulin *et al.* (1997). The retrieved onset dates account for the whole ecosystem phenology at the landscape level, and include, in principle, tree canopies and understorey plants.

We adjusted the leaf onset dates from 8 km to our 0.5° model resolution, using our modified version of the DISCover land covermap. The onset date at 0.5° resolution is obtained by averaging the data for the 8 km pixels covered by the dominant biome at 0.5° resolution. At the 0.5° resolution, the retrieved onset dates over the period 1983–93 show that 79% of the pixels exhibit interannual variation of onset date of less than 10 days, a value lower than the satellite temporal resolution. Moreover, within any given biome, the spatial variability of the onset dates among 0.5° pixels is generally larger than the interannual variability within each 0.5° pixel. That legitimizes the

Table 1 Subdivision of biomes as defined by the DISCover land-cover map. Δ_T, T_c, and T_{mean} are, respectively, the annual range, the coldest, and the annual mean of daily mean air temperature. The number of 0.5° pixels (NbP) does not include those where the algorithm of Moulin *et al.* (1997) fails to detect an onset date. *, areas for which we model the phenology (95% of unmasked 0.5° pixels)

Biome criteria (°C)	Subdivision	NbP	Region
Cool evergreen needleleaf forest	$T_{mean} < 10$	3475*	Bor.
Warm evergreen needleleaf forest	$T_{mean} \geq 10$	205	Tropical
Cool deciduous needleleaf forest/Woodland		1859*	Bor.
Cool deciduous broadleaf forest	$T_{mean} < 15$	903*	Temp.
Warm deciduous broadleaf forest	$T_{mean} \geq 15$	285	Tropical
Cool mixed forest	$T_c < 0$	3982*	Bor./Temp.
Warm mixed forest	$T_c \geq 0$	123	Tropical
Cool closed shrubland	$Tc < 0$	859*	Arct./Bor.
Warm closed shrubland	$T_c \geq 0$	343	Tropical
Cool open shrubland	$\Delta_T > 20$ or $T_c < 5$	947*	Bor./Temp.
Warm open shrubland	$\Delta_T \leq 20$ and $T_c \geq 5$	389	Tropical
Cool woody savannah	$T_c < 0$	3722*	Arct./Bor.
Warm woody savannah	$T_c \geq 0$	1635*	Tropical
Warm savannah		2483*	Tropical
Cool grassland	$\Delta_T > 20$ or $T_c < 5$	2780*	Temp.
Warm grassland	$\Delta_T \leq 20$ and $T_c \geq 5$	618*	Tropical
Cool permanent wetland	$T_c < 0$	908*	Bor./Temp.
Warm permanent wetland	$T_c \geq 0$	13	Tropical
Cool crop/Natural vegetation mosaic	$T_{mean} < 15$	3346*	Temp.
Warm crop/Natural vegetation mosaic	$T_{mean} \geq 15$	1510*	Tropical

computation of a temporal average of the onset dates over the entire NDVI 1983–93 period, with the exception of years 1991 and 1992, which are corrupted by the screening of aerosols emitted by the Pinatubo eruption (Vermote *et al.* 1994). Therefore, we excluded these two years to produce mean satellite onset dates over the 1983–93 decade. Finally, we ignored those 0.5° pixels where our algorithm failed to detect an onset date for at least one year; these occurred primarily in transition zones between evergreen and deciduous tropical forests.

The spatiotemporal scatter of onset date within a 0.5° pixel generates an overall standard deviation σ_μ, that we decompose into two terms. First, we compute the spatiotemporal standard deviation σ of onset date within 0.5°. If we assume that the 8-km pixel onset dates within a 0.5° pixel are independent, the uncertainty is divided by the square root of n, the number of observed onset dates over the study period (the maximum of n is 50 8-km pixels times 9 years). However, this latter assumption may underestimate σ_μ because adjacent 8-km pixels do not have independent edaphic and climatic conditions. Therefore, the uncertainty due to spatiotemporal scattering is between σ and $\sqrt{\sigma^2/n}$. Secondly, uncertainty arises from the time-resolution of the NDVI time series. The maximum composite NDVI of the Pathfinder dataset is the highest daily value over 10 days, in order to minimize clouds attenuation. This sampling produces an error that is not reduced by the subsequent averaging over the 0.5° pixel (σ_{sat}). We estimate σ_{sat} from the standard deviation of a square 10-day wide distribution, as given by:

$$\sigma_{sat}^2 = \int_0^{10} \frac{x^2}{10} dx - \left(\int_0^{10} \frac{x}{10} dx \right)^2 = 8.33 \text{ days}^2. \quad (1)$$

The overall variance (σ_μ^2) is then given by:

$$\sigma_\mu^2 = \frac{\sigma^2}{n} + \sigma_{sat}^2. \quad (2)$$

In summary, the spatial distribution of the onset dates at 0.5° resolution is shown in Fig. 2, and the pertaining uncertainties (σ_μ) in Fig. 3. Large values of σ_μ are obtained in the several dry areas and within rapid transition zones between different biomes (e.g. mountains). In such areas, the subgrid heterogeneity of climate is great, and so the mean onset date is meaningless. Thus, in the water-controlled zone we have excluded open shrublands and closed shrublands; in the temperature controlled zone, we have excluded permanent wetlands, deciduous broadleaf forests, and mixed forests. Figure 1(b) shows the biomes for which we have attempted to model phenology.

Global climate and soil moisture fields

Our leaf onset models require two input climate data: air temperature or soil moisture. The climate data were derived from the ERA-15 reanalysis of the European

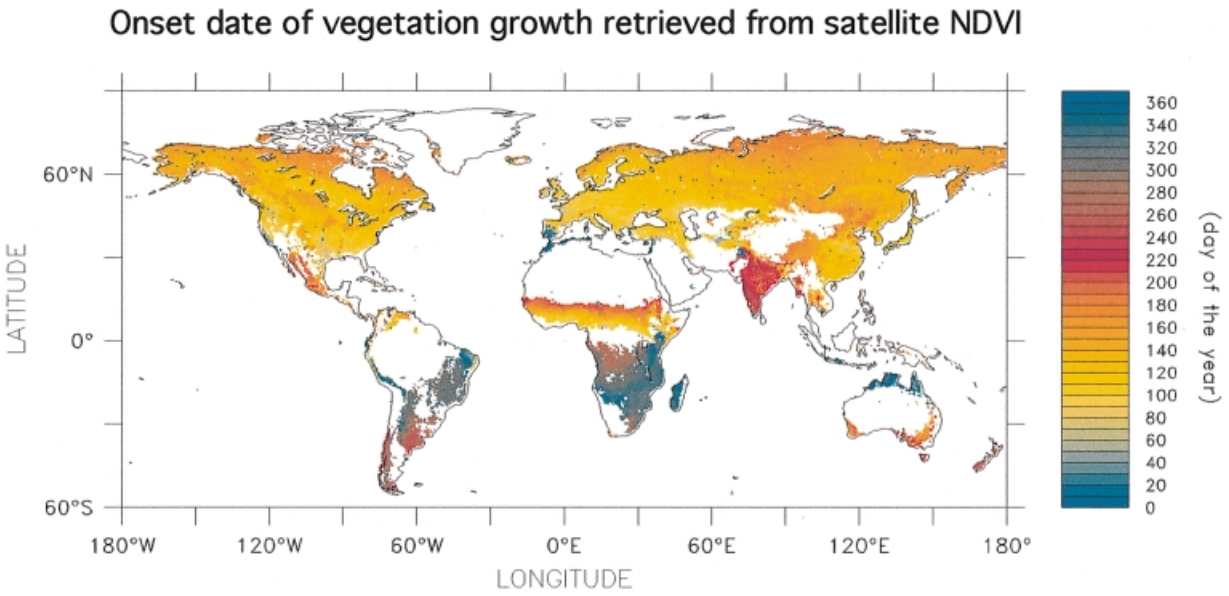

Fig. 2 Spatiotemporal mean of leaf onset dates at 0.5° resolution for 1983–90 and 1993 retrieved from AVHRR composite NDVI. We first computed the onset date at 8-km resolution for each of the nine years using an algorithm derived from Moulin *et al.* (1997). The mean value at 0.5° resolution over the whole time period is then defined, including only the 8-km pixels covered by the dominant biome at 0.5°. Areas where our algorithm fails to detect an onset date from the NDVI signal at least for one year are shown in white.

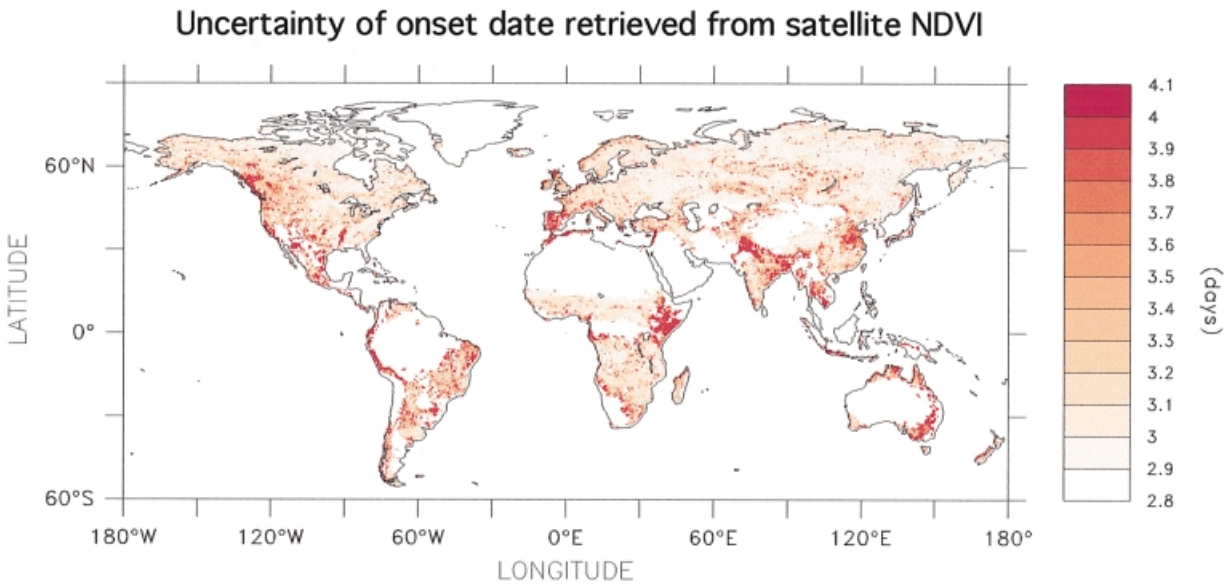

Fig. 3 Uncertainty of the satellite-derived onset date at 0.5° of Fig. 2. This uncertainty is due to the spatiotemporal aggregation (nine years and a maximum of 49 8-km pixels) and to the satellite sampling of 10 days.

Center for Medium-Range Weather Forecasts (ECMWF) model, available at a 1° spatial resolution over the study time period (Gibson *et al.* 1996). Reanalysis involves assimilating, at each 6-h time-step of a global weather forecast model, a set of ground and satellite meteorological observations to correct the model deviations. Daily mean air temperature is taken directly from ECMWF model reanalysis. As the reanalysis of rainfall is less reliable, we have corrected the data with 5° monthly rainfalls from NCDC (regridded at the ECMWF resolution; Bissinger 1992; Eischeid *et al.* 1995; Gibson *et al.* 1997). Daily rainfalls are obtained by applying the average daily variability of the ECMWF rainfall to the monthly NCDC data. Soil moisture is then computed using the land-surface scheme SECHIBA (Ducoudré *et al.* 1993), forced by the corrected ECMWF reanalysis climate

fields. The relative soil moisture (*rsm*), the relevant variable for phenology, depends on the soil type through the wilting point (*wilt*) and field capacity (*fc*) values:

$$rsm = \frac{asm - wilt}{fc - wilt}, \quad (3)$$

where *asm* is the absolute soil moisture.

Models of leaf onset

The onset of vegetation growth is controlled either by abiotic factors, such as climate or soil type, or by biotic factors, in a manner analogous to endogenous control or competition between species. At the spatial resolution of available globally gridded climate data, biotic factors would be very difficult to model. Fortunately, with the exception of tropical rain forests they are not predominant in controlling the leaf onset date (Reich 1994).

The physiological processes involved in triggering leaf onset are still not fully understood. Models ordinarily use one of two main approaches. A few studies have computed leaf onset based on the optimization of resources (Kindermann *et al.* 1993; Kikuzawa 1995), but most adopt an empirical approach using bioclimatic factors to define the climate factors that limit leaf onset (e.g. drought, light, or frost). We follow the second approach as being the more common in the literature. The first step is the identification of limiting factor(s) for leaf onset for each biome. Temperate deciduous forest is the most studied biome. Several models of leaf onset date based on temperature have been developed. Earlier works have assumed that the parameters controlling bud development are related linearly to temperature. For instance, according to de Réaumur (1735), leaf onset occurs when the sum of average daily temperature above a given threshold, accumulated from a starting date (1 January) reaches a prescribed value. Later experiments have identified the need to incorporate other factors such as light and chilling conditions, which influence the temperature dependency of leaf onset (Vegis 1964; Garber 1983). Some models have determined the thermal control on leaf onset using the duration of the photoperiod, since longer days promote the onset of vegetation (Nizinski & Saugier 1988), and different strategies have been developed to introduce chilling requirements (Sarvas 1972; Cannell & Smith 1986; Hari & Häkkinen 1991; Hänninen 1994). When applied in a range of sites, however, more sophisticated models do not necessary produce better results (Hunter & Lechowicz 1992)*.

*For more details about phenological models of temperate deciduous forest see Kramer (1996).

Very few studies have been carried out on leaf onset in other natural biomes. Over boreal and arctic regions, soil frost is likely to be the principal factor delaying the onset of vegetation, by controlling water availability in permafrost areas (Bertrand *et al.* 1994; Waelbroeck *et al.* 1997). Grassland phenology is controlled both by soil moisture and temperature depending upon the particular climatic regime (Dickinson & Dodd 1976; Pitt & Wikeem 1990; Stewart & Dwyer 1994). In the tropical savannahs and seasonal tropical forests, the principal factor is soil moisture, although other variables like soil type can also play a role (Farrar *et al.* 1994; Le Roux 1995).

We have selected only those phenological models that require input data at the global scale. Such models are either applied directly, or adapted where necessary, in order to have at least one model for each biome. Overall, we have chosen six models to apply to the different biomes.

Model 1: boreal and arctic biomes. The end of soil frost is estimated from the accumulated 'growing days', since reliable soil temperature data are not available. The number of growing days (*NGD*), defined as the number of days during the preceding two months on which the daily mean air temperature is above a certain threshold ($T_{th} = -5\,^{\circ}C$), is the phenology-driving parameter. Leaf onset occurs when *NGD* exceeds a critical set value (NGD_c), determined by the model.

Models 2a and 2b: temperate and boreal biomes. The effect of temperature on leaf onset is estimated using 'growing degree days' (*GDD*). We sum the daily mean air temperature above an arbitrary threshold ($T_{th} = -5\,^{\circ}C$ or $0\,^{\circ}C$, according to the biome) for a fixed period of time ($N = 10$, 20 or 30 days). Leaf onset occurs when *GDD* reaches a critical value (GDD_c). In model 2a, GDD_c is fixed, whereas in model 2b GDD_c decreases with the photoperiod *P* (Nizinski & Saugier 1988). The three parameters (*a*, *b* and *c*) are determined with the following equations:

$$GDD(t) = \sum_{t-N}^{t} Max(T - T_{th}, 0) \text{ and } GDD(t) \geq GDD_c \quad (4)$$

$$GDD_c = a \text{ for model 2a} \quad (5)$$

$$GDD_c = \frac{bP}{cP - 1} \text{ for model 2b.} \quad (6)$$

Model 3: boreal and temperate biomes. This model combines heat and chill requirements assuming that an increase in chilling days reduces the plant's *GDD* demand (Cannell & Smith 1986; Murray *et al.* 1989). A chilling day has a daily mean air temperature below a

particular threshold ($T_{th} = 0\,°C$ or $5\,°C$ depending on the biome). We use the method of Murray *et al.* (1989), starting summation from fixed dates: 1 November for the number of chilling days (NCD_{Nov}) to cover the major part of the dormant period, and 1 January for growing degree days (GDD_{Jan}). In this study, the cool biomes are exclusively in the Northern Hemisphere; the use of fixed dates is then possible. The onset date occurs when the observed GDD_{Jan} exceeds a critical value, which is an exponential function of NCD_{Nov}. We thus have to determine three parameters (a, b and c), according to the following equations:

$$GDD_{Jan}(t) = \sum_{Jan1}^{t} Max(T - T_{th}, 0) \quad (7)$$

$$\text{and } GDD_{Jan}(t) \geq a + b^{*}e^{(c^{*}NCD_{Nov}(t))} \text{ with } c < 0. \quad (8)$$

Models 4a and 4b: tropical biomes. Adopting the approach of Le Roux (1995), model 4a determines a critical value of relative soil moisture that initiates vegetation growth. Relative soil moisture is defined in the description of the climate dataset above. Because results from SECHIBA runs are used for the soil moisture field, only the first metre of the soil column is considered in this estimation. Model 4b assumes that leaf onset lags behind the accumulation of water in the soil, the lag being specific for each biome. We estimate the onset date of the soil hydrological cycle (D) as the first 5-day period, from 1 January for Northern Hemisphere and from 1 July for the Southern Hemisphere, with increasing soil moisture. However, we need to filter out small rises of soil moisture, not sufficient to trigger a leaf onset detectable by satellite. For the 25 days after D, the number of days with increasing soil moisture is required to be greater than the number of days with decreasing soil moisture. The time lag between D and the leaf onset date is parameterized. Because model 4b does not employ a fixed value of relative soil moisture, it can represent regional adaptation to soil type or orographic influence at the model scale.

Determination of phenological model parameters

Method

For each biome, we used satellite leaf onset dates and climatic data to retrieve the observed spatial distribution of the model parameters (e.g. NGD_c or GDD_c). The method of calibration used depends on the kind of model:

- We estimate the constant parameter (model 1, 2a, 4a and 4b) as the main mode (X) of the frequency distribution of the observations, and calculate its standard deviation (σ_X). When no mode can be identified, we reject the model for the studied biome. White *et al.* (1997) estimate the optimal parameter by minimizing the difference between observed and simulated onset dates. However, we will demonstrate on an example (below) that our method is more appropriate for isolating multiple modes and for filtering out atypical data.
- For models based on a relationship between two variables (model 2b and 3), we plot the variables for all 0.5° pixels belonging to the biome, and apply a least-squares fit regression. The uncertainty of each parameter is also calculated. We reject the model if r^2 is lower than 0.5, to ensure that the relationship reproduces at least 50% of the variability of the observed signal.

Results

Distinct biomes may have identical parameterizations regardless of the model used. This was the case for models 1 and 2a over cool closed shrubland and cool woody savannah (Tables 2 and 3). We attribute this to the similar phenological behaviour of the biomes, which are usually aggregated into a single biome often called 'tundra' in other classification schemes (Haxeltine & Prentice 1996). We also found similar NGD_c parameter values for cool deciduous needleleaf forest/wood, cool mixed forest and cool permanent wetland (Table 2). As displayed in Fig. 4, we aggregated these three biomes and defined a common NGD_c of 15 days. A simple linear average of the NGD_c distribution would yield a NGD_c of 23 days, while minimizing the difference between observed and simulated onset dates would yield a NGD_c of 21 days. Those methods capture the mean behaviour of the entire biome, but ignore the existence of a dominant mode of phenological functioning.

We managed to define model 1 parameters for arctic and boreal biomes only by using the arbitrary threshold of –5 °C (Table 2). Arctic biomes (cool woody savannah and cool closed shrubland) require larger NGD_c to initiate their growing season than boreal biomes (25 and 15 days, respectively). We interpret this to be a consequence of a longer soil thawing period in the arctic. Some biomes exhibit spatially heterogeneous phenological behaviours, e.g. cool evergreen needleleaf forests. Figure 5 shows two primary modes: one for North America ($NGD_c = 14$ days) and the other for Northern Europe ($NGD_c = 23$ days) This bimodal behaviour is likely due to climatic differences between the two continents. North America has a more continental climate, with colder winters than northern Europe (colder T_{mean} and T_c).

Biome	T_{th} (°C)	NGD_c (days)
Cool evergreen needleleaf forest (Europe)	−5	23 ± 13
Cool evergreen needleleaf forest (America)	−5	14 ± 28*
Cool closed shrubland	−5	25 ± 14
Cool woody savannah	−5	25 ± 14
Cool deciduous needleleaf forest/Woodland	−5	15 ± 18*
Cool permanent wetland	−5	15 ± 18*
Cool mixed forest	−5	15 ± 18*

Table 2 Global-scale calibration of the model 1, the critical number of growing days (NGD_c) is estimated by the main value (X) and the scatter (σ_X) of the observed distribution of this parameter ($NGD_c = X \pm \sigma_X$). Some biomes show asymmetric scattering of NGD_c around X (*)

Biome	T_{th} (°C)	GDD_c (°C*days)
Cool closed shrubland	−5	125 ± 68
Cool woody savannah	−5	125 ± 68
Cool deciduous broadleaf forest	0	180 ± 72
Cool crop/Natural vegetation mosaic	0	135 ± 80
Cool grassland	−5	240 ± 113
Cool open shrubland	−5	200 ± 93

Table 3 Global-scale calibration of the model 2a, the critical value of growing degree days (GDD_c) is estimated as NGD_c in Table 2

Model 2a appears suited to predict the leaf onset date for arctic and temperate biomes using arbitrary thresholds of –5 °C and 0 °C, respectively (Table 3). However, it shows no dominant mode for boreal forests. The calibration of model 2b yields no result for any of the biomes, including the cool deciduous broadleaf forest biome for which it was originally developed at the local scale. This suggests that while such a model may be accurate at the local scale, it does not provide a good description of the leaf onset date at a larger scale. *GDD* and photoperiod of 0.5° pixels covered by this biome computed using the same counting period ($N = 10$ days) as Nizinski & Saugier (1988) are plotted in Fig. 6(a). The field observations used by Nizinski and Saugier and the associated fit are also shown. Clearly, the local model cannot be scaled up as no relationship is observed between the two variables. There are several reasons why the extrapolation of model 2b fails. First, the observations of Nizinski and Saugier are from Fontainebleau forest in France, which is covered by croplands at the 0.5° pixel resolution. Secondly, in order to evaluate the spatial heterogeneity of phenology within a biome, we isolated the 0.5° pixels corresponding to the scattered points surrounding the local data (Fig. 6a), which are all the American cool deciduous broadleaf forests. But even in these regions, we could not fit a curve (with $r^2 > 0.5$). Thirdly, the onset dates derived from satellite NDVI correspond to 25% of greenness of the whole biome, while the field observations are real first flushing dates of oak trees. Lastly, it seems that even within the cool deciduous broadleaf forests there is a large heterogeneity in the phenological response to photoperiod. Hunter & Lechowicz (1992) have shown that photoperiod is less efficient than heat and chilling requirements for phenology prediction in temperate deciduous forests when applied to different sites.

For the cool deciduous broadleaf forests, we instead apply model 3 using $T_{th} = 5$ °C, as in Murray *et al.* (1989). Murray *et al.* isolated five relationships between NCD_{Nov} and GDD_{Jan}, according to tree species. Figure 6(b) shows only the two extreme curves and our global observations of GDD_{Jan} vs. NCD_{Nov}. In this case, most of the 0.5° pixels follow the same relationship as in Murray *et al.* It is then possible to compute an exponential fit to the observations (Table 4).

Model 4a could not be calibrated in the tropics. A fixed value of relative soil moisture does not seem to be able to trigger leaf onset in water controlled areas. This could be a result of soil/plant adaptations, and to the local heterogeneity of soil moisture (e.g. drainage basin). It could also be a consequence of the inaccuracy of the simulated soil moisture field. However, we were able to calibrate model 4b in all water controlled regions. For cool evergreen needleleaf forests, it was necessary to distinguish two behaviours for warm savannah according to the hemisphere (Table 5). The reasons for this dichotomy in phenological behaviour are still uncertain.

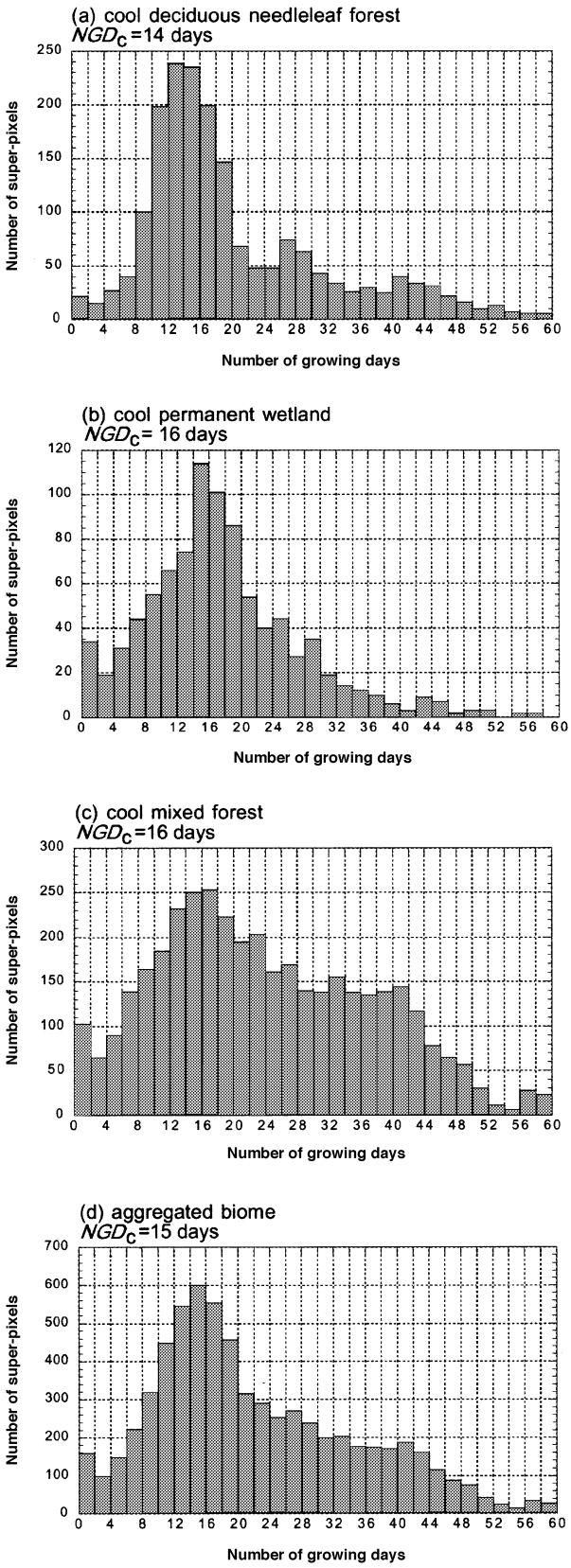

Fig. 4 Common behaviour of cool deciduous needleleaf forest/woodland, cool permanent wetland and cool mixed forest using model 1. These three biomes present a main mode in their frequency distribution of observed NGD_c of approximately 15 days.

Spatial goodness-of-fit of the models

The second step of this study was to run the different biome/model associations with the climate dataset used for calibration, in order to estimate the quality of the fit. For each biome/model association, we tested whether the relationship resulting from the first mode of the frequency distribution adequately represented the spatial distribution of onset dates within the biome. We also estimated the sensitivity of each model to its parameters uncertainties. Then, using two statistical criteria, we selected the best model for each biome in our global unified model, and analysed the spatial performance.

Model sensitivity to parameter uncertainty

In the calibration step, an uncertainty (σ_X) was computed for each model parameter (X). For models with a threshold (model 1, 2a, 4b), we estimate the shift of the simulated onset date averaged over the whole biome produced by adding or subtracting σ_X to X. For model 3, which uses three parameters, we define the upper and lower curves by combining the uncertainties. Then, we use the two extreme curves to compute the mean shift on the simulated onset date. Results are presented in Table 6. In the water controlled regions, the parameter uncertainty is linked linearly to the model performances (values in Tables 6 and 5 are the same). However, this is not the case in temperature-controlled regions, where all the models contain thresholds or nonlinear relationships between variables. Consequently, for a given model, a biome with a low parameter uncertainty could also have a large uncertainty in onset prediction. For model 2a, the parameter of the cool crops/natural vegetation mosaics and cool grasslands are defined, respectively, with 80 and 113 degree-days, but the derived onset uncertainty is of a similar magnitude (+16/–20 and +16/–23 days, respectively). Furthermore, adding or subtracting the uncertainty does not give symmetrical deviation in the simulated onset date. For the cool grassland–model 2a association, increasing the GDD_c of 110 degree-day led to an onset delay of +16 days, whereas decreasing it by the same value led to an onset delay of –23 days.

Selection of the best model for each biome

The root mean-square of observed vs. simulated onset date (RMS) and the linear correlation coefficient (ρ) for each biome/model association, are given in Table 7 for temperature-controlled regions and in Table 8 for water-controlled regions. These values are computed considering only 0.5° pixels where a model successfully simulates an onset. A model may fail to find an onset date for several 0.5° pixels because the requirements are never, or are always, fulfilled. In the case where more than one model is calibrated for a single biome, we compute RMS and ρ over the subset of 0.5° pixels where all models predict an onset date. This allows us to compare model performances with the same dataset (Table 7). The best biome/model associations are emphasized in bold in Tables 7 and 8.

In general, temperature-controlled regions have lower RMS than water-controlled regions; the vegetation onset date of temperature-controlled biomes is simulated between 9 to 31 days, compared with 42 to 89 days for water-controlled biomes. However, ρ can be equally high (0.80 compared to 0.78) in both regions. Figure 7 illustrates this apparent paradox, by showing observed vs. simulated onset dates for a temperature- and a water-controlled biome (cool permanent wetland and warm savannah). The range in warm savannah onset dates is clearly much larger than the range in cool permanent wetland onset dates. Thus, warm savannah can show a higher ρ despite a quite large RMS. Therefore, ρ is not a good estimator of model reliability for biomes like cool permanent wetlands, which have a narrow range of onset dates.

For cool deciduous broadleaf forest, model 2a appears to be the best choice (the lowest RMS and the highest ρ). However, if we compare RMS and ρ obtained with the common dataset, model 3 appears to be more appropriate. Besides, model 2a underestimated the earliest onset dates and overestimates the latest ones (Fig. 8). Model 3 best reproduces most onset dates, but computes extremely unrealistic onset dates for 5% of the biome. Nevertheless, these few anomalous results have a disproportionate effect on RMS and ρ. We isolated the pixels with onset dates greater than 160 (day of the year); they all occurred on the border between temperate and tropical areas, where water availability influences the leaf

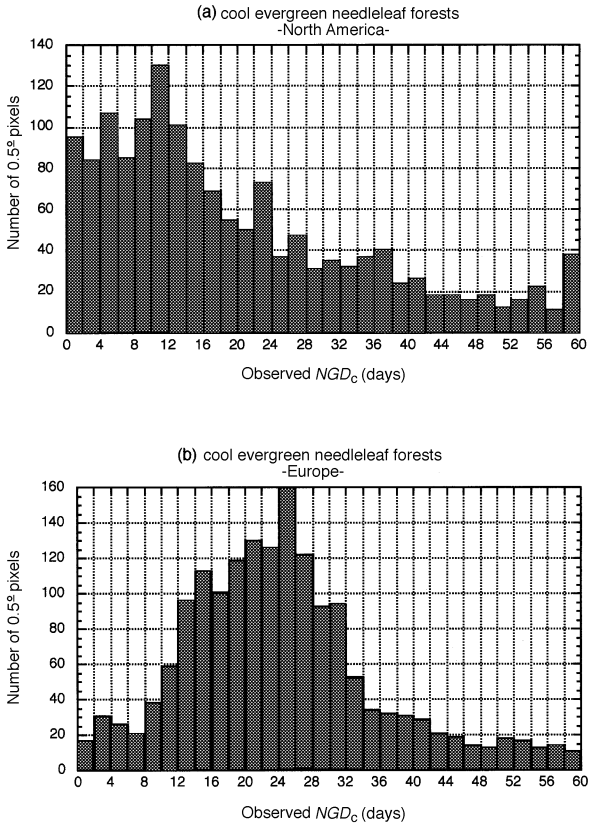

Fig. 5 Different phenological behaviours within the cool evergreen needleleaf forest biome according to climatic regime. The leaf onset growth of the cool evergreen needleleaf forest occurs with less NGD over the two previous months (14 days) in North America than in Europe (23 days).

Table 5 Global-scale calibration of the model 4b. The critical time-lag between the onset of the soil hydrological cycle and the vegetation cycle (Time-lag) is estimated as NGD_c in Table 2

Biome	Time-lag (days)
Warm woody savannah	50 ± 41
Warm crop/Natural vegetation mosaic	75 ± 78
Warm grassland	45 ± 95
Warm savannah (NH)	70 ± 41
Warm savannah (SH)	40 ± 43

Table 4 Global-scale calibration of the model 3: its parameters, their associated and the square of the coefficient of linear correlation between observed and estimated *GDD* (r^2)

Biome	T_{th} (°C)	*a*	*b*	*c*	r^2
Cool deciduous broadleaf forest	5	−68 ± 22	638 ± 16	−0.010 ± 0.001	0.59

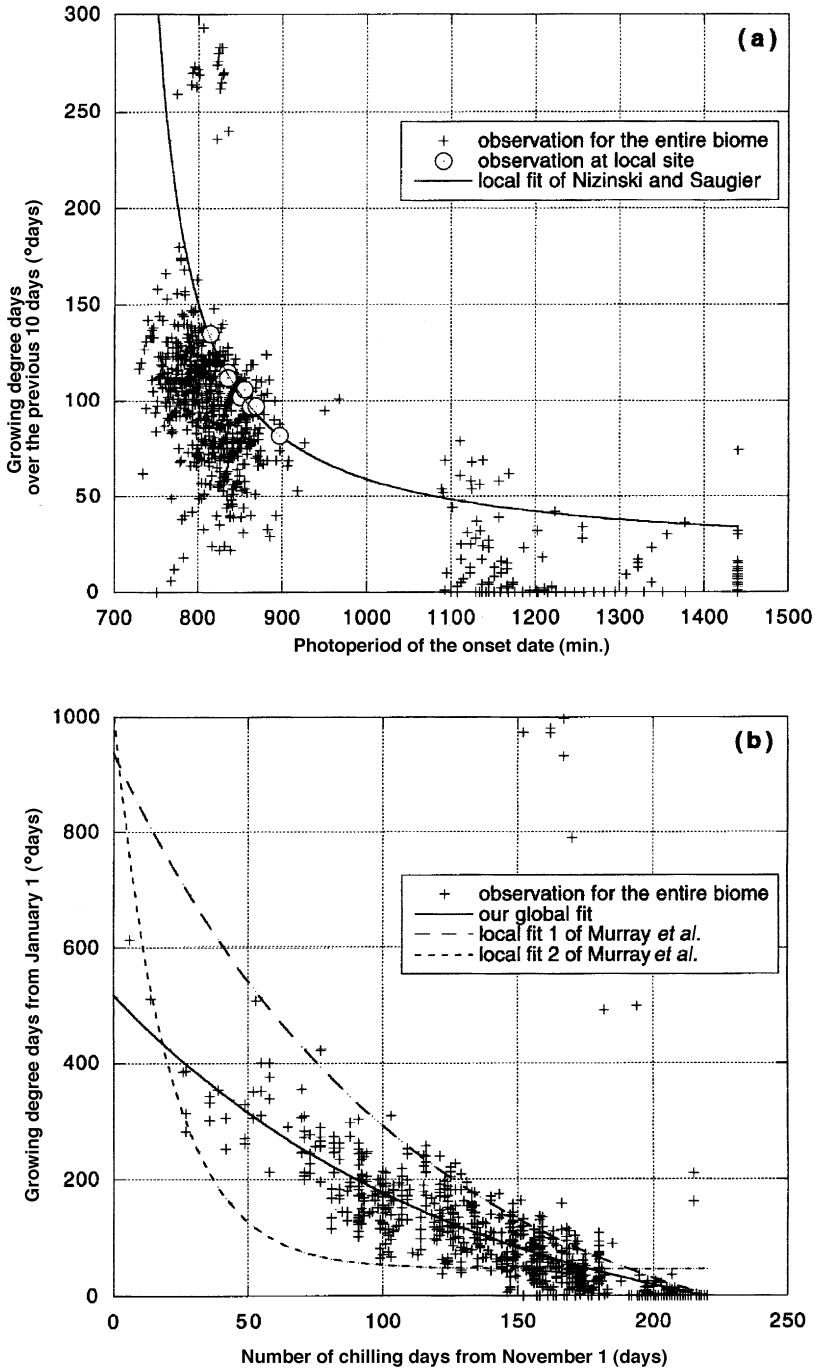

Fig. 6 Extrapolation of two local phenological models at the global scale for cool deciduous broadleaf forest. (a) Nizinski & Saugier (1988): dots and crosses represent local and global observations, respectively, and the line is the fit derived from the local observations (b) Murray *et al.* (1989): dashed curves represent the spread of the local fits, and crosses again represent global observations. The scatter plot of the observations (crosses) shows the same trend as the local fits (dashed curves). The line is the selected global fit.

onset as well as temperature. Thus, we retain model 3 for this biome. For cool closed shrubland and cool woody savannah, we selected model 2a rather than model 1.

Spatial predictions of the unified model

In general, the unified model obtained by selecting the best biome/model association simulates onset dates realistically. The primary spatial gradients , including the aridity gradient in the Sahel and the frost gradient in the Northern Hemisphere, are well represented (Fig. 9). Figure 10 exhibits the difference between the simulated and the satellite-retrieved onset dates. The difference is not computed where the unified model is unable to simulate an onset date. Because we have selected the average behaviour for each biome, atypical areas are not represented so well. Thus, the results for each biome depend on the scatter of fitted parameters and the

Table 6 Model sensitivity to parameter uncertainties, mean bias on simulated onset date introduced by adding or subtracting the uncertainty σ_X on each parameter (in days)

	Prediction uncertainty (days)			
Biome	Model 1	Model 2a	Model 3	Model 4
Cool evergreen needleleaf forest (Europe)	+11/–12			
Cool evergreen needleleaf forest (America)	+10/–14			
Cool deciduous needleleaf forest/Woodland	+13/–17			
Cool deciduous broadleaf forest		+12/–18	+17/–5	
Cool mixed forest	+13/–17			
Cool closed shrubland	+14/–13	+11/–8		
Cool open shrubland		+19/–22		
Cool woody savannah	+14/–13	+11/–8		
Warm woody savannah				+41/–41
Warm savannah (NH)				+41/–41
Warm savannah (SH)				+43/–43
Cool grassland		+16/–23		
Warm grassland				+95/–95
Cool permanent wetland	+13/–17			
Cool crop/Natural vegetation mosaic		+16/–20		
Warm crop/Natural vegetation mosaic				+78/–78

Table 7 Global results of different biome/model associations in the temperature-controlled region: ρ, correlation coefficient; RMS, root mean-square between observed and simulated onset date (in days); NbP, number of 0.5° pixels where model simulates an onset date. Bold characters indicate the retained biome/model associations. Asterisks indicate ρ and RMS values computed on 0.5° pixels where all the models calibrated for a given biome simulate an onset date

	Model 1			Model 2a			Model 3		
Biome	ρ	RMS	NbP	ρ	RMS	NbP	ρ	RMS	NbP
Cool evergreen needleleaf forest	**0.58**	**12**	**2734**						
Cool dec. needleleaf forest/Wood.	**0.34**	**12**	**1848**						
Cool dec. broadleaf forest				0.31	22	849	**0.19**	**31**	**899**
				0.31*	22*	849*	**0.58***	**18***	**849***
Cool mixed forest	**0.51**	**15**	**3591**						
Cool closed shrubland	0.58	14	763	**0.58**	**17**	**876**			
	0.64*	14*	716*	**0.80***	**11***	**716***			
Cool open shrubland				**0.76**	**20**	**876**			
Cool woody savannah	0.38	10	3595	**0.50**	**24**	**3678**			
	0.51*	10*	3571*	**0.70***	**9***	**3571***			
Cool grassland				**0.65**	**24**	**2548**			
Cool permanent wetland	**0.61**	9	**893**						
Cool crop/ Natural vegetation mosaic				**0.49**	**20**	**3120**			

nonlinearity models. For example, cool deciduous broadleaf forests are well represented (shown in grey in the Fig. 10). Areas below the curve in Fig. 6(a) have a late simulated onset date with respect to the satellite observations, and areas above the curve have an early simulated onset date. The unified model fails to predict an onset date in several 0.5° pixels covered by the cool mixed forest in Quebec and the US. As shown in Fig. 4(c), these areas have a NGD_c larger than 15 days, so the heat requirement defined by our model is always satisfied. This biome, by definition, has a mixed species composition, which may explain our difficulty to select a unique model. The same problem occurs for the cool grasslands in Tibet, where the heat requirement of model 2a is never fulfilled. Areas with a large uncertainty in the satellite observation (Peru or the north of India) also exhibited a large discrepancy between observed and simulated onset dates (Figs 3 and 10).

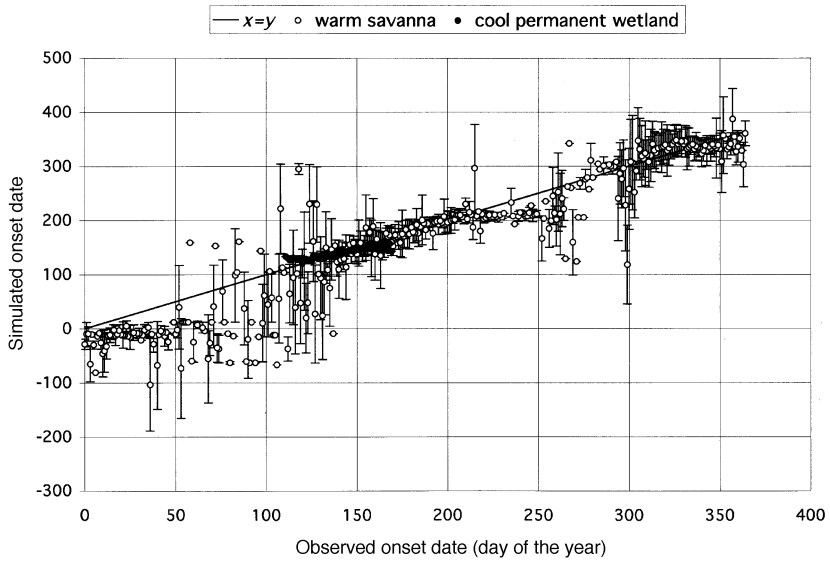

Fig. 7 Observed vs. simulated onset dates for warm savannah and cool permanent wetland. Simulated onset dates range from –200–600 to account for the 365-day cycle of calendar.

Table 8 Global results of different biome/model associations in the water-controlled region (same legends as Table 7). All correlation coefficients are significant, warm grassland and warm crop/natural vegetation mosaic excepted

	Model 4b		
Biome	ρ	RMS	NbP
Warm woody savannah	0.67	42	1670
Warm savannah	0.78	42	2470
Warm grassland	0.06	89	611
Warm crop/Natural vegetation mosaic	0.09	66	1506

Discussion

The calibration method does not consider uncertainty in the satellite observations. Biomes with larger error bars on satellite onset dates have higher parameter uncertainties and hence larger uncertainties in the predicted onset date. In the future, weights could be applied to the observations, determined by the uncertainty in the curve-fitting procedure.

Some assumptions made in the land-surface scheme SECHIBA may also have an impact on our model performance. First, SECHIBA uses a potential land-cover map obtained by the model BIOME1 (as described in Prentice *et al.* 1992), whereas we use the DISCover land-cover map. For instance, South-east Asia is covered by evergreen/warm mixed forest in the BIOME1 distribution, and by crop/natural vegetation mosaic in the DISCover map. In such regions, the soil moisture computed by SECHIBA deviates significantly from reality. Secondly, SECHIBA does not account for land-use change and practice (irrigation), which may affect the soil water conditions. Lastly, the root zone depth is assumed to be one metre, independent of the biome.

Discrepancies in some regions (e.g. Brazil) could be due to the low frequency of satellite observations. In most of these areas, the intense cloudiness prevents the detection of an onset date for at least one year of the satellite record. We suspect that, even in other years, the cloudiness may perturb the NDVI signal, and the detection algorithm may return a meaningless onset date.

The NDVI data (originally at 8-km resolution) may present an important heterogeneity within a single 0.5° pixel. The phenological processes responsible for this subgrid heterogeneity of onset dates are not the same in dry and wet regions. In dry areas like West Africa, vegetation is sparse and generally responds to subgrid hydrological events (local rainfall). In wet areas such as central Africa, vegetation phenology can be controlled predominantly by plant genetics (Reich 1995). Furthermore, a given species may change its strategy against water stress. In Israel, *Quercus ithaburensis* is able to become 'evergreen' depending on the climate conditions (Ne'eman 1993). Singh & Singh (1992) have shown that the seasonal cycle of adjacent Indian plants may be asynchronous under severe water stress. Besides, Borchert (1994) has demonstrated that soil moisture is not sufficient to represent plant water availability; physiological characteristics such as water reserve or specific soil structure are also important. Finally, it is still not clear whether it is possible to reproduce the tropical vegetation phenology without accounting for the subgrid variability of the hydrology. In temperate and high latitudes, the subgrid heterogeneity is less important and leaf phenology is driven mainly by temperature. Temperature is far less spatially heterogeneous than

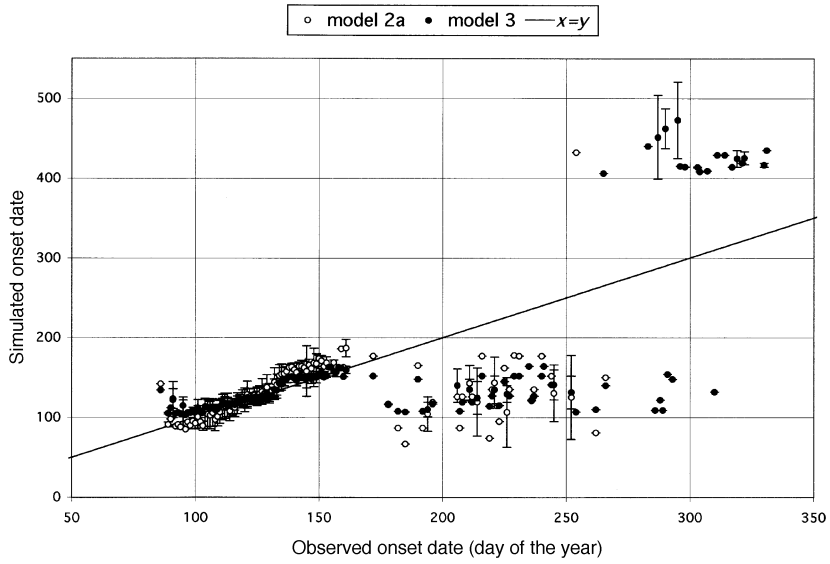

Fig. 8 Comparison of model 2a and model 3 performances for cool deciduous broadleaf forest. Simulated onset dates range from 0 to 600 (see Fig. 7).

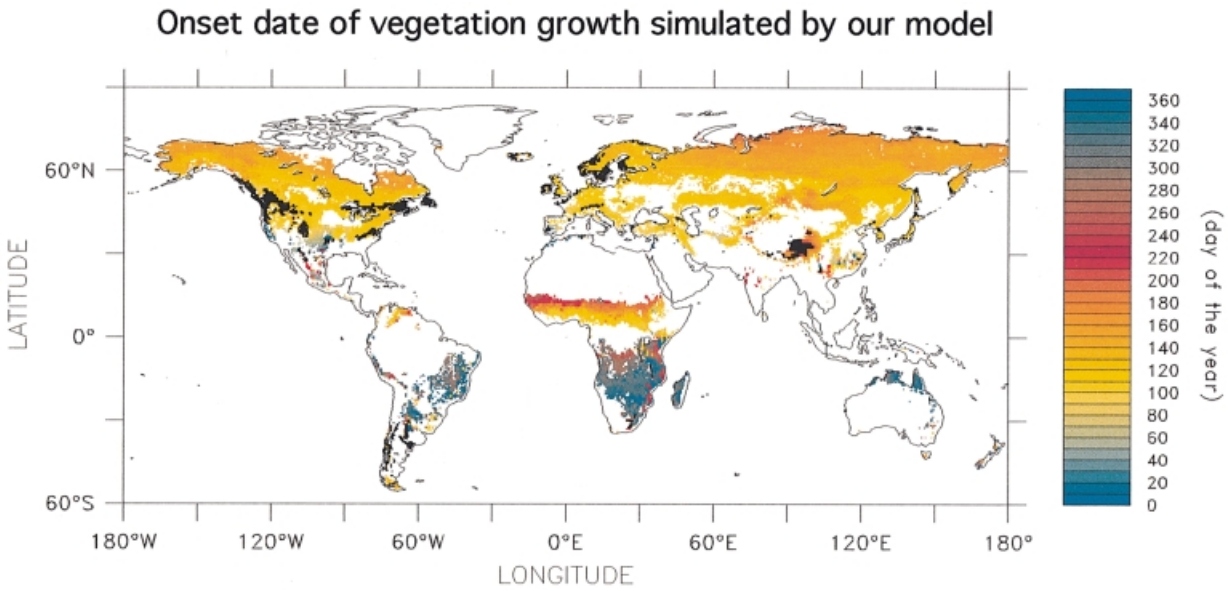

Fig. 9 Leaf onset dates simulated by our global unified model at 0.5° resolution. Areas where our model fails to simulate an onset are shown in black.

precipitation. This scaling issue is also present in mountainous regions (the Rockies and the Himalayas), where we lack the subgrid climatology typical of these regions to reproduce their phenology accurately.

Conclusion

This study shows that the extrapolation of local phenological models to the global scale is not trivial. Variables that reflect local adaptation (in particular, photoperiod) are not relevant at the global scale. Nevertheless, we have successfully defined a unified phenological model for all the natural deciduous biome areas. Our model reproduces the leaf onset date for 62% of the temperature-controlled regions within 10 days of the satellite onset date, and for 75% within 15 days (Fig. 11). The phenology of water-controlled regions is more difficult to simulate. Only 32% of the water-controlled regions have a simulated onset date within the 10-day satellite resolution, and 75% are within 43 days. There are three possible causes for the larger error in our model in water-controlled areas (tropics and subtropics): the instrumental limitations of the satellite due to cloudiness near the intertropical convergence

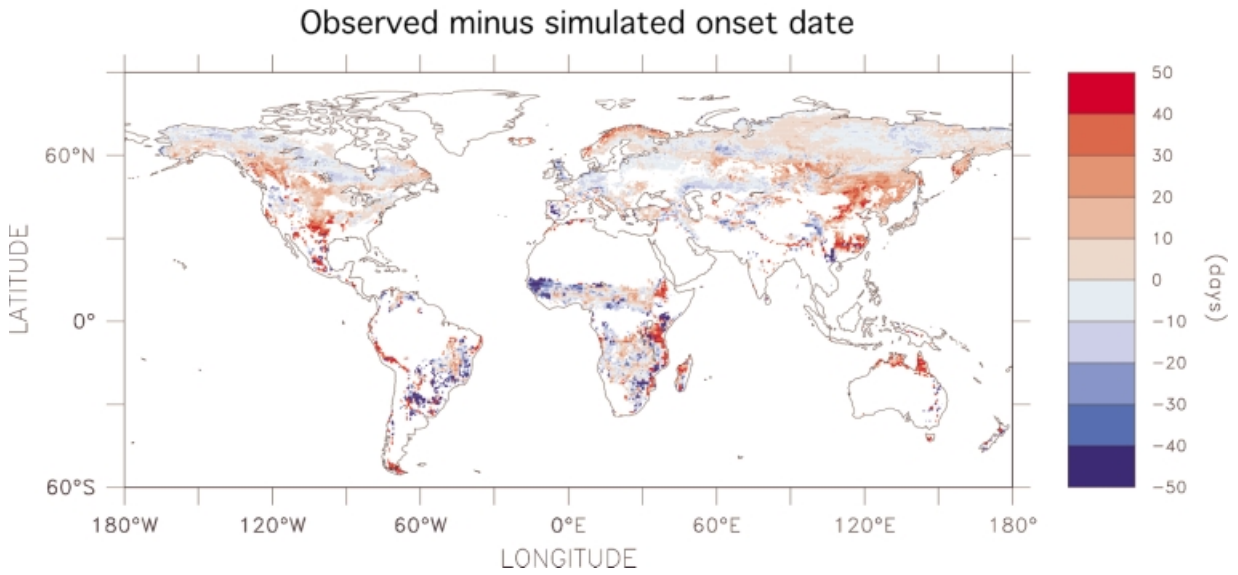

Fig. 10 Spatial distribution of observed minus simulated onset dates. Areas in white are either, excluded biomes, 0.5° pixels where our model fails to simulate an onset, or 0.5° pixels where our algorithm fails to detect an onset date in the NDVI records. The differences range from −183 to 183 days to account for the 365-day cycle of the calendar.

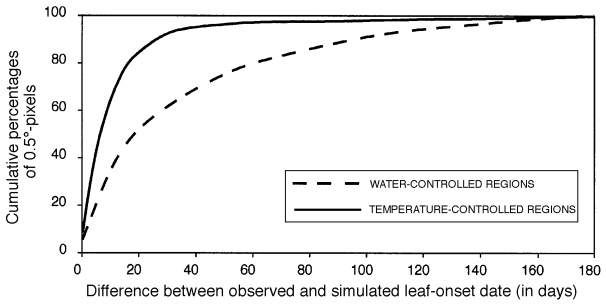

Fig. 11 Histogram of cumulated frequencies of absolute difference between observed and simulated leaf onset dates.

zone, the low reliability of input data (rainfall and soil moisture), and the importance of subgrid processes. When we normalized the onset date differences by the observation error, the range of error became more similar for both temperature- and water-controlled regions. Additionally, the relative spatial heterogeneity of the onset date was reproduced similarly in the two regions. However, the higher variability in the tropics leads to a higher absolute error. To adequately simulate the tropical leaf onset date, it may be essential to reproduce the subgrid hydrological processes. It is unclear whether a mean value can be used in regions with a high subgrid heterogeneity, and whether a model based on ecological requirements at the local scale (8 km) can simulate the average of a larger region (0.5°).

If we assume that spatial and temporal variations are controlled by the same physical processes, then we could use our unified model to study interannual variability of phenology. However, the model accuracy is of the same order as the interannual variability of the leaf onset date (15 days in mid and high latitudes and 60 days in the tropics), and so it may be difficult to reproduce this signal. Nevertheless, our phenological model can be viewed, within a given biome, as the asymptotic (or long-term) response to climate change from one location to another one. Thus, our model could be used to reproduce large temporal variability such as the decadal trends observed in the NDVI (Myneni *et al.* 1997; Menzel & Fabian 1999), or in the vegetation activity itself (Goulden *et al.* 1996; Botta 1999), and possibly part of the response to El Niño events.

Acknowledgements

We thank the following bodies for providing data for this study: the Earth Observing System Pathfinder Program of NASA's Mission to Planet Earth in collaboration with National Oceanic and Atmospheric Administration, The Earth Observing System Data and Information System (EOSDIS), Distributed Active Archive, the AVISO vent-flux data centre of Meteo France for the ECMWF Reanalysis data. This research was supported with funds from the French Commissariat à l'Energie Atomique.

References

Bertrand A, Robitaille G, Nadeau P, Boutin R (1994) Effects of soil freezing and drought stress on abscisic acid content of sugar maple sap, leaves. *Tree Physiology*, **14,** 413–425.

Betts RA, Cox PM, Lee SE, Woodward FI (1997) Contrasting physiological and structural vegetation feedback in climate change simulations. *Nature*, **387,** 796–799.

Bissinger R (1992) The global Climate Perspectives System (GCPS): The Hardware/Software Component. In *Eighth International Conference on Interactive Information and Processing Systems for Meteorology, Oceanology, and Hydrology,* Atlanta GA.

Borchert R (1994) Soil and stem water storage determine phenology and distribution of tropical dry forest trees. *Ecology*, **75** (5)**,** 1437–1449.

Botta A (1999) *Modélisation globale de la phénologie de la biosphère continentale à partir de données satellitaires.* PhD thesis, Université Pierre et Marie Curie, Paris.

Cannell MJR, Smith RI (1986) Climatic warming, spring budburst and frost damage on trees. *Journal of Applied Ecology*, **23,** 177–191.

Chase TN, Pielke RA, Kittel TGF, Nemani R, Running SW (1996) Sensitivity of a general circulation model to global changes in leaf area index. *Journal of Geophysical Research*, **101** (D3)**,** 7393–7408.

Dickinson CE, Dodd JL (1976) Phenological patterns in a short grass prairie. *American Midland Naturalist*, **96,** 367–378.

Ducoudré NI, Laval K, Perrier-Sechiba A (1993) A New Set of Parameterization of the Hydrologic Exchanges at the Land–Atmosphere Interface within the LMD Atmospheric General Model. *Journal of Climate*, **6,** 248–273.

Eischeid JK, Baker CB, Karl TR and Diaz HF (1995) The quality control of long-term climatological data using objective data analysis. *Journal of Applied Meteorology*, **34,** 2787–2795.

Farrar TJ, Nicholson SE, Lare A (1994) The influence of soil type on the relationships between NDVI, rainfall, and soil moisture in semiarid Botswana. II. NDVI response to soil moisture. *Remote Sensing and Environement*, **50,** 121–133.

Friend AD, Stevens AK, Knox RG, Cannell MGR (1997) A process based terrestrial biosphere model of ecosystem dynamics (HYBRID v3.0), *Ecological Modelling*, **95,** 249–387.

Garber MP (1983) Effects of chilling and photoperiod on dormancy release of container-grown loblolly pine seedlings. *Canadian Journal of Forest Research*, **13,** 1265–1270.

Gibson JK, Källberg P, Uppala S, Hernandez A, Noumura A, Serrano E (1997) *ECMWF* Re-Analysis Project Report Series, 1. ERA Description, *Technical Report ECMWF*, Reading, UK, 1997. viii, 72 pp.

Gibson R, Källberg P, Uppala S (1996) The ECMWF Re-analysis (ERA) Project. *ECMWF Newsletter*, **73,** 7–17.

Goulden ML, Munger JW, Fan SM, Daube BC, Wofsy SC (1996) Exchange of carbon dioxide by a deciduous forest: Response to interannual climate variability. *Science*, **271,** 1576–1578.

Hänninen H (1994) Effect of climatic change on trees from cool and temperate regions: an ecophysiological approach to modelling of bud burst phenology. *Canadian Journal of Botany*, **73** (2)**,** 183–199.

Hari P, Häkkinen R (1991) The utilization of old phenological time series of bud burst to compare models describing annual cycles of plants. *Tree Physiology*, **8,** 281–287.

Haxeltine A, Prentice IC (1996) BIOME3: an equilibrium terrestrial biosphere model based on ecophysiological constraints, resource availability and competition among plant functional types. *Global Biogeochemical Cycles*, **10** (4)**,** 693–709.

Hunter AF, Lechowicz MJ (1992) Predicting the timing of budburst in temperate trees. *Journal of Applied Ecology*, **29,** 597–604.

Justice CO, Townshend JRG, Holben BN, Tucker CJ (1985) Analysis of the phenology of global vegetation using meteorological satellite data. *International Journal of Remote Sensing*, **6** (8)**,** 1271–1318.

Kaduk J, Heimann M (1996) A prognostic phenology scheme for global terrestrial carbon cycle models. *Climate Research*, **6,** 1–19.

Kikuzawa K (1995) Leaf phenology as an optimal strategy for carbon gain in plants. *Canadian Journal of Botany*, **73,** 158–163.

Kindermann J, Lüdeke MK, Badeck F *et al.* (1993) The Frankfurt Biosphere Model (FBM). *Water Soil, and Air Pollution*, **70,** 675–684.

Kramer K (1996) *Phenology and growth of European trees in relation to climate change.* PhD thesis, Wageningen University, The Netherlands.

Le Roux X (1995) *Etude et modélisation des échanges d'eau et d'énergie sol-végétation-atmosphère dans une savane humide.* PhD thesis, Université Pierre et Marie Curie, Paris.

Lieth H (1975) *Primary Productivity of the Biosphere*, pp. 237–264. Ecological Studies. Springer, Berlin.

Loveland TR, Belward AS (1997) The IGBP-DIS global 1km land cover data set, discover: first results. *International Journal of Remote Sensing*, **18** (15)**,** 3289–3295.

Menzel A, Fabian P (1999) Growing season extended in Europe. *Nature*, **397,** 659.

Moulin S, Kergoat L, Viovy N, Dedieu G (1997) Global scale assessment of vegetation phenology using NOAA/AVHRR satellite measurements. *Journal of Climate*, **10,** 1154–1170.

Murray MB, Cannell GR, Smith RI (1989) Date of budburst of fifteen tree species in Britain following climatic warming. *Journal of Applied Ecology*, **26,** 693–700.

Myneni RB, Keeling CD, Tucker CJ, Asrar G, Nemani RR (1997) Increased plant growth in the northern latitudes from 1981 to 1991. *Nature*, **386,** 698–702.

Ne'eman G (1993) Variation in leaf phenology and habit in *Quercus ithaburensis*, a Mediterranean deciduous tree. *Journal of Ecology*, **81,** 627–634.

Nizinski JJ, Saugier B (1988) A model of leaf budding and development for a mature quercus forest. *Journal of Applied Ecology*, **25,** 643–652.

Pitt MD, Wikeem BM (1990) Phenological patterns and adaptations in a *artemisia/ agropyron* plant community. *Journal of Range Management*, **43** (4)**,** 350–367.

Prentice ICW, Cramer SP, Harrison R, Leemans RA, Monserud, Solomon AM, A (1992) global biome model based on plant physiology and dominance, soil properties and climate. *Journal of Biogeography*, **19,** 117–134.

de Réaumur RAF (1735) Observations du thermomètre, faites à Paris pendant l'années 1735, comparées à celles qui ont été faites sous la ligne, à l'Isle de France, à Alger et en quelques-unes de nos isles de l'Amérique. *Mémoire de l'Académie des Sciences, Paris*, 545 pp.

Reich PB (1994) Phenology of tropical forests: Patterns, causes, and consequences. Canadian. *Journal of Botany*, **73,** 164–174.

Rouse JW, Haas RH, Schell JA, Deering DW, Harlan JC (1974) Monitoring the vernal advancement of retrogradation of natural vegetation. NASA/GSFC Type III Final Report, Greenbelt M.D. 371 pp.

Ruimy A, Dedieu G, Saugier B (1996) TURC: a diagnostic model

of continental gross primary productivity and net primary productivity. *Global Biogeochemical Cycles*, **10** (2), 269–285.

Sarvas R (1972) Investigations on the annual cycle of development of forest trees. Active period. *Communicationes Instituti Forestalis Fenniae*, **76** (3), 110.

Sellers PJSO, Los CJ, Tucker CO *et al.* (1996) revised land surface parameterization (SiB2) for atmospheric GCM: Part II the generation of global fields of terrestrial biospherical parameters from satellite data. *Journal of Climate*, **9** (4), 706–737.

Singh JS, Singh VK (1992) Phenology of seasonally dry tropical forest. *Current Science*, **63** (11), 684–689.

Stewart DW, Dwyer LM (1994) A model of expansion and senescence of individual leaves of field-grown maize (*Zea mays* l.). *Canadian Journal of Plant Science*, **74 (1),** 37–42.

Townshend JRG (1994) Global data sets for land applications from the Advanced Very High Resolution Radiometer: an introduction. *International Journal of Remote Sensing*, **15,** 3319–3332.

Vegis A (1964) Dormancy in Higher Plants. *Annual Review of Plant Physiology*, **5,** 185–222.

Vermote E, Saleous NE, Kaufman YJ, Dutton E (1994) Data preprocessing: startospheric aerosol perturbing effect on the remote sensing of vegetation: correction method for the composite NDVI after the Pinatubo eruption. In *6th international symposium on physical measurements and signatures in remote sensing*, 151–158, Val d'Isère, France.

Viovy N, Arino O, Belward AS (1992) The Best Index Slope Extraction (BISE): A method for reducing noise in NDVI time-series. *International Journal of Remote Sensing*, **13** (8), 1585–1590.

Waelbroeck C, Monfray P, Oechel WC, Hasting S, Vourlitis G (1997) The impact of permafrost thawing on the carbon dynamics of tundra. *Geophysical Research Letters*, **24** (3), 229–232.

White MA, Peter E, Thornton E, Running SW (1997) A continental phenology model for monitoring vegetation responses to interannual climatic variability. *Global Biogeochemical Cycles*, **11** (2), 217–234.